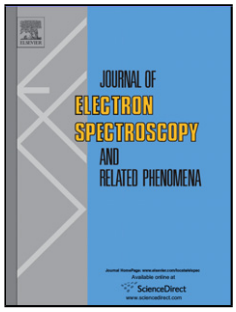

Title: Effective attenuation length of keV photoelectrons in silicon measured by transmission through thin membranes

Authors: Vladyslav Solokha, Tien-Lin Lee, Axel Wilson, Kurt Hingerl, Jörg Zegenhagen

PII: S0368-2048(17)30272-4
DOI: https://doi.org/10.1016/j.elspec.2018.03.003
Reference: ELSPEC 46745

To appear in: *Journal of Electron Spectroscopy and Related Phenomena*

Received date: 21-11-2017
Revised date: 6-3-2018
Accepted date: 7-3-2018

Please cite this article as: Vladyslav Solokha, Tien-Lin Lee, Axel Wilson, Kurt Hingerl, Jörg Zegenhagen, Effective attenuation length of keV photoelectrons in silicon measured by transmission through thin membranes, Journal of Electron Spectroscopy and Related Phenomena https://doi.org/10.1016/j.elspec.2018.03.003

Effective attenuation length of keV photoelectrons in silicon measured by transmission through thin membranes

Vladyslav Solokha[a,b], Tien-Lin Lee[a], Axel Wilson[a], Kurt Hingerl[b] and Jörg Zegenhagen[a*]

[a] *Diamond Light Source Ltd, Harwell Science and Innovation Campus, Didcot, Oxfordshire, OX11 0DE, UK*

[b] *Johannes Kepler Universität Linz, Altenberger Straße 69, 4040 Linz, Österreich*

[*] *Corresponding author, e-mail address: jorg.zegenhagen@diamond.ac.uk*

Highlights

Hard X-ray photoelectron spectroscopy (HAXPES) measurements are becoming increasingly popular for investigating buried objects (interfaces, inclusions, dopants, stacked electronic materials, etc.), but experimental data for material properties such as electron attenuation lengths, which are necessary for an associated careful data analysis, are still scarce. To this extend, we present new data for the effective attenuation length of electrons in silicon in the energy range from ~ 2 to 10 keV, which we obtained using a novel approach that is particularly useful for electrons with a kinetic energy in the (multi) keV range.

We also underline and provide evidence that HAXPES in combination with thin membranes will be a very useful technique for studying materials under (near) ambient conditions when exploiting the high brilliance of advanced, modern synchrotron radiation sources.

Last not least, in a direct comparison we find that the chemical shift of the Si and Al core levels is surprisingly - and against intuition - larger for the higher binding energy 1s than the shallower 2s and 2p core levels.

Abstract

We use 9nm and 15nm thin membranes for determining the effective attenuation length of photoelectrons in silicon. One side of silicon membranes was covered with a thin film of aluminium and exposed to X-rays with energies from 3 to 8 keV. We recorded Al 1*s* and 2*s* photoelectrons that were (a) emitted from the Al film directly and (b) transmitted through the membranes. With the help of the ratio of both yields, we obtained values for the effective attenuation length (EAL) of electrons with kinetic energies up to 7.9 keV in silicon. The experimentally determined EAL values are smaller than obtained

from different predictive equations. Using a power law fit $EAL\,(k,p) = kE_{kin}^{p}$ to the experimental and predicted EAL values we find that mainly different is the pre-factor of the power law, k, while the exponent, i.e. the dependence on kinetic energy E_{kin} is represented well. Our study underlines the feasibility of using membranes for investigating surfaces under (near) ambient pressure conditions by photoelectron spectroscopy and points out the advantages of employing hard X-rays.

Keywords: photoelectron spectroscopy; effective attenuation length; membranes; thin films; synchrotron radiation; X-rays

1 Introduction

Photoelectron spectroscopy (PES) is a well-established powerful technique providing valuable information about the electronic properties, chemistry and structure of materials. While every photo-excited electron emerging from the sample carries useful information, the so called elastic electrons, which did not lose energy in collisions, are of particular interest. The flux of elastic electrons observed from a specific photo-excited element of a buried object depends on the probability of the photoexcited electrons to escape the material without energy loss. In practical applications (e.g. film thickness determination) a parameter used to describe the probability of escape is the effective attenuation length (EAL) of the electrons. The EAL depends on the electron kinetic energy, the material traversed by the electrons and the used geometry. It is an important parameter for the exact quantitative characterization of the structure of materials by photoelectron spectroscopy (PES). For the exact quantitative structural and chemical characterization of micro- and nano-structures as well as thin films and interfaces, which are presently in the focus of interest, accurate values for EAL are needed as a function of electron kinetic energy.

Of course, the flux I_{pe} of emitted photo electrons (PEs) depends on the photoelectric cross section σ_{PE}, which strongly depends on the specific element and electronic orbital. Values for the cross sections have been calculated comprehensively, e.g., by Scofield [1, 2]. Since cross sections decrease dramatically with excitation energy E_Y (roughly, $\sigma_{PE} \sim E_Y^{-3}$), PES studies were for a long time carried out mostly using moderate photon energies, i.e., within the ultraviolet and up to the soft/tender X-ray range (E_Y <(<) 2 keV). Hence, over the years, most of the EAL data has been collected for photoelectrons with kinetic energies in that range. Comprehensive data are available, e.g. from the National Institute of Standard and Technology (NIST) [3] regarding electron elastic scattering cross sections, the inelastic mean free path (IMFP), the effective attenuation length (EAL) and other useful parameters.

The EAL of electrons is determined by the inelastic scattering and elastic scattering of the electrons. The inelastic mean-free-path (IMFP) of a photoelectron is the mean distance that an electron travels in a specific material before it undergoes an inelastic collision and is thus lost from the elastic channel. Electrons with kinetic energy E_{Kin} suffer energy loss (ΔE), in the order of probability, by plasmon excitation ($\Delta E \approx$ 10 eV), phonon excitation ($\Delta E <$ 1 eV), excitations of core electrons with binding energy $E_B < E_{Kin}$ ($\Delta E = E_B$) and Bremsstrahlung ($\Delta E \leq E_{Kin}$). The IMFP depends on the atomic numbers Z of the elements in a material but much less than e.g. X-ray attenuation lengths. For electron kinetic energies above about 100 eV and all elements from lithium (Z = 3) to bismuth (Z = 83) the difference in IMFP is less than an order of magnitude [4].

The probability that an electron is able to travel within a material from a point A to B without energy loss is further reduced by elastic scattering. Elastic collisions, which change the direction (k-vector) of the electron without energy transfer, are dominated by scattering by the (screened) Coulomb potential of the heavy core. Differential elastic scattering cross-section can be calculated using Dirac-Hartree-Fock method [5]. Because of elastic scattering in the material electrons do not travel along a straight-line, thus having an increased probability of inelastic scattering. The elastic scattering also modifies the angular distribution of photoelectrons. For electrons escaping the material both effects combined, generally, lead to EAL being shorter than IMFP for electrons escaping at an angle up to about ≈60° with respect to the surface normal whereas EAL may be even longer than IMFP for even larger angles [6]. This non-intuitive fact is a result of the definition of the EAL by the International Organisation for Standardisation: "Parameter when introduced in place of the IMFP into an expression derived for AES and XPS on the assumption that elastic-scattering effects are negligible for a given quantitative application, will correct that expression for elastic-scattering effects" [7].

It is self-evident that the depth from which an electron is escaping from the material depends on the electron emission angle α with the surface normal. For a specific material the mean escape depth (MED) equals EAL if the electron is emitted normal to the surface (α = 0). For various reasons [7], which we do not want to discuss in detail here, the angular

dependence is not described by a simple 1/cos(α) relationship for larger α. For some more information on MED, IMFP and EAL of electrons, we suggest consulting a brief review that was recently published by Powell and Tanuma [7].

The drastic decrease in the photoelectric cross sections with photon energy mentioned above can only be compensated by a corresponding boost in photon flux. Highly brilliant third-generation synchrotron light sources are becoming increasingly available and hard X-ray PES (HAXPES) has become continuously more popular over the last decade [8, 9, 10] for investigating true bulk properties or deeply buried objects [11]. Extending the analytic power of PES into the (multi-) keV range requires accurate values for the EAL in this energy range as well, which motivated the present study. The availability of more experimental EAL values will also allow testing existing numerical approximations and phenomenological predictions for the EAL in this energy range. To this extent, we are presenting here a novel approach to obtain EAL values in the (multi) keV range by determining the transmission of photoelectrons through thin silicon membranes [12].

We should note already here that for using this approach the measurement of the EAL can be affected by the oxidation of the membrane material and surface contaminations. Oxygen atoms chemically reacting with the membrane increase the number of scattering centres. Therefore, values of the EAL of the silicon membrane obtained without accounting for its oxidation will underestimate the electron EAL in the pure material. Useful for future exploitation of this method, a detailed discussion of the effect of these contaminations is found in Section 3.2. It turns out that that the overall uncertainties introduced by these contaminations are small.

The present study is also motivated by another reason. There are numerous studies published for applying the analytical power of PES to investigating surfaces under (near) ambient conditions [13]. However, the contradicting requirements of operating the sample at high pressure while keeping the necessary vacuum conditions for the electron analyser impose serious restrictions on the experimental set up. Using thin membranes for such applications may help. In particular combined with HAXPES, we believe that membranes might be useful for separating the delicate photoelectron analyzer hardware and electronics from harsh environments.

2 Experimental

The experiments were performed on the I09 beamline at the Diamond Light Source Ltd (DLS). X-ray excitation energies E_Y of 3, 4, 6 and 8 keV were selected by a Si(111) monochromator. Photoelectron spectra were acquired using a VG Scienta EW4000 HAXPES concentric hemisphere analyzer (CHA) equipped with a 70 frame/sec CCD camera as electron detector.

For the study we employed commercially available (TEMwindows.com) 0.1 × 1.5 mm^2 size silicon membranes with two thicknesses d_{mem}, i.e. 9 and 15 nm. The membranes are supported on a 0.1 mm thick silicon substrate with a diameter of 3 mm as schematically shown on the right hand side of Fig. 1(a). On the face where the membrane was flush with the substrate membrane and substrate were covered with aluminium (in vacuum, base pressure $2x10^{-6}$) by e-beam evaporation with the substrates held at room temperature. The film thickness, d_{film} = 22 nm, was measured by a profilometer.

For the method which we employed for determining the EAL, it was necessary to have two membranes covered with an Al film of identical thickness. To assure this, two substrates with membranes of the same thickness were deposited simultaneously side by side with Al. With 22 nm the Al film thickness was chosen thin enough such that it was illuminated homogeneously over the whole thickness with the same X-ray intensity even for the lowest X-ray energy used (3 keV), i.e. that absorption of the X-rays in the film could be neglected. As will become clear from the following, slight differences in the thickness of these two silicon membranes would not affect the accuracy of the results. The covered samples were stored under ambient conditions for several weeks prior to the experiments. The structure of the samples which we used is shown schematically in Fig. 1(a).

Such a pair of membranes was mounted side by side on a high precision manipulator in a way that in one case the Al film and in the other case such membrane was facing the photoelectron analyzer as shown schematically in Fig. 1(b). In the first case, the Al photoelectrons excited in the thin film are reaching the CHA directly and in the second case they have to penetrate the Si membrane first.

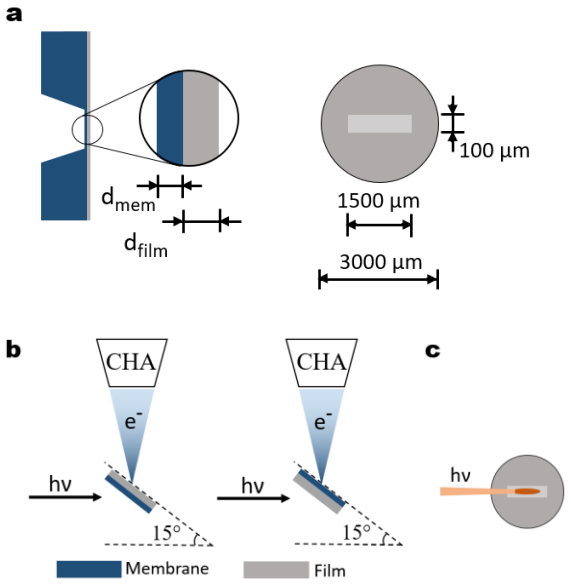

Figure 1. (a) Schematic of aluminium coated Si membranes where d_{mem} and d_{film} are the thicknesses of the membrane and the Al film respectively. (b) Schematic top views of the two experimental geometries with film (grey) and membrane (dark blue) facing the lens-entrance of the photoelectron analyzer (CHA). Both Al films had been deposited side by side and were thus of the same thickness. (c) Sketch of the 40 × 40 µm^2 beam incident at an angle of 15° with respect to the surface plane positioned in the middle of the membrane.

The X-ray beam was focused to a size of 0.04×0.04 mm^2 to assure that the area illuminated by the beam was significantly smaller than the size of the membrane, as indicated in Fig. 1(c). With the help of the Al photoelectron signal, the membranes were positioned such that the beam was hitting their center. At an X-ray energy of 3 keV, Al photoelectrons could only be detected when the beam was hitting the membrane since the 0.1 mm silicon substrate not only absorbed the emitted photoelectrons completely but also most of the incoming X-rays. Even at the highest X-ray energy (8 keV) and 15° angle of incidence the X-ray transmission of the 0.1 mm silicon substrate is only 0.3 % which allowed easy determination when the beam hit the membrane since the Al signal is enhanced by a factor of 300. On the other hand, the absorption of the X-rays in the 9 or 15 nm Si membrane can be neglected. With the precision manipulator the samples were then positioned such that the beam was aligned to the center of the membrane (cf.

Fig. 1c). X-ray polarization vector, sample surface normal and CHA were in the horizontal plane. (cf. Fig. 1b).

For both membrane thicknesses we recorded spectra for four X-ray energies for the two cases shown in Fig, 1(b), i.e. with the Al film of sample one facing the CHA and with the Si membrane of sample two facing the analyzer. The measuring time and all other parameters were identical for both measurements. The beam position was kept constant with µm accuracy with the help of a beam position monitor and a feedback system. Because DLS operates in the so-called top-up mode with a constant electron beam current (usually 300 mA) the X-ray beam intensity stayed constant.

3 Results

3.1 Determination of the effective attenuation length of electrons in the silicon membrane

For the determination of the effective attenuation length of electrons in the silicon membrane we used photoelectrons with two different binding energies E_B, namely Al 1*s* and 2*s* (E_{b1s} = 1559.6 eV and E_{b2s} = 117.8 eV). Figure 2 shows spectra of the region around Al 2s recorded with Al facing the analyzer (Fig 2a) and with the 15nm Si membrane facing the analyzer (Fig 2b). The ratio of the (1*s* or 2*s)* Al photoelectron yield recorded with the membrane facing the analyzer Y_m to the yield recorded with the Al facing the analyzer Y_{Al} is a direct measure of the transmission T of the membranes for the 1*s* or 2*s* photoelectrons with the corresponding kinetic energies $E_{kin} = E_\gamma - E_B$, i.e. $T = Y_m / Y_{Al}$.

The yields Y_m and Y_{Al} were obtained for the used excitation energies by extracting the integral of the Al 1s and Al 2*s* photoelectron peaks from the spectra using a pseudo Voigt function with Shirley background subtracted. Transmission values for the lowest kinetic energy (E_{kin} ≈ 1440 eV) were obtained by analysing the Al 1*s* photoelectrons excited by 3 keV photons. With excitation energy of 8 keV the Al 2*s* photoelectrons provided the transmission values for the highest electron kinetic energy (E_{kin} ≈ 7.88 keV).

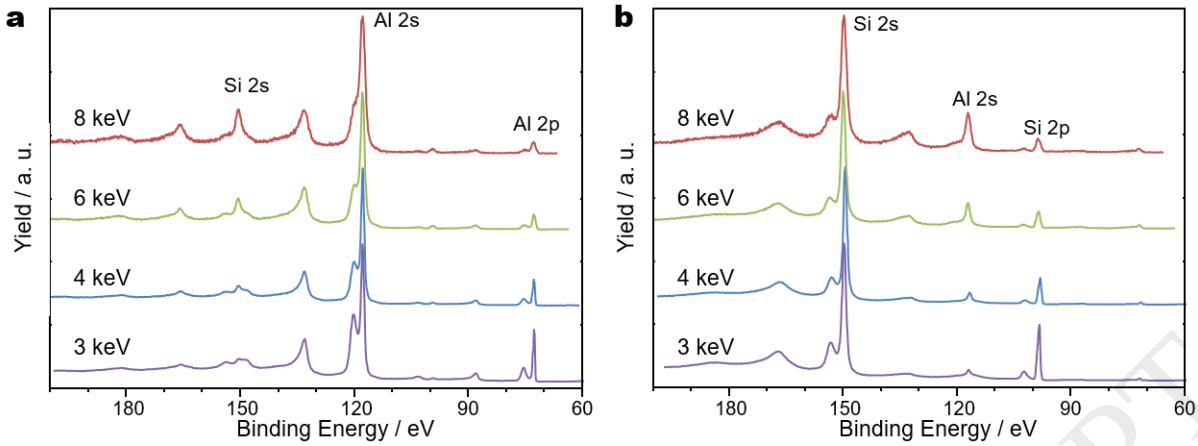

Figure 2. Photoelectron spectra of the Al 2s region measured at 3, 4, 6 and 8 keV excitation energy for the sample with 15 nm Si membrane shown on a linear scale with (a) the Al film facing the analyzer and (b) the Si membrane facing the analyzer (cf. Fig. 1). The spectra recorded for 4, 6 and 8 keV are vertically offset for clarity. All spectra in (a) and (b) are normalized to the Al 2*s* and Si 2*s* peaks, respectively and shown on a linear scale.

The peak extraction for Al 2*s* was slightly complicated, due to the Si 2*p* peak having an overlap with the Al 2*s* peak with the first plasmon produced by Si 2*p* (Fig 3).

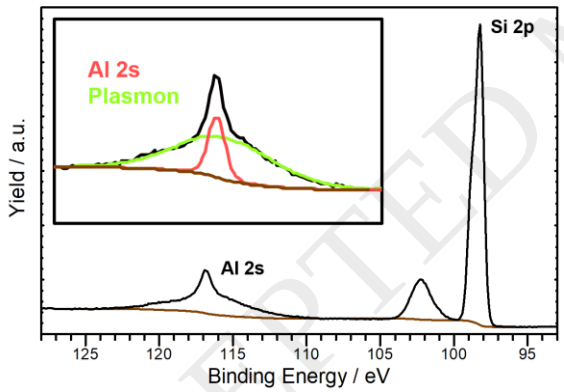

Figure 3. Al 2s peak and the neighbouring Si 2p at E_Y = 3 keV for membrane to analyzer geometry. The inset shows a close up view of Al 2s region with a fit of Al 2s elastic peak (red) and Si plasmon of Si 2p (green).

We estimated the Si 2*p* plasmon intensity by assuming that the relative Si 2*s* plasmon intensity $\frac{Y^{pl}_{Si2s}}{Y^{el}_{Si2s}}$, where Y^{pl} is the plasmon intensity and Y^{el} is the intensity of the elastic peak, is the same as for Si 2*p*. This assumption is justified, since the

scattering cross-section for plasmon excitation by electrons in a specific material is a function of the electron kinetic energy, but it is only weakly energy dependent. The difference in the kinetic energies of Si 2*s* and Si 2*p* photoelectrons is small, therefore the magnitude of the Si 2*p* plasmon can be estimated as

$$Y_{Si2p}^{pl} = Y_{Si2p}^{el} \frac{Y_{Si2s}^{pl}}{Y_{Si2s}^{el}} \qquad (1).$$

Subtracting this contribution from the total area, formed by the Al 2*s* peak plus the Si 2*p* plasmon (cf. Fig.3), and removing additionally the Shirley-background gives the net Al 2*s* electron yield. Attempting to extract the Al 2*s* yield by peak fitting gave similar results but was less trustworthy because of difficulties fitting the shape of the Si 2*s* plasmon peak, and thus determining the Al 2*p* intensity reliably.

Calculating T with the help of the thus obtained Y_m and Y_{Al} data, the effective attenuation length of the photoelectrons, L, traveling through the membrane is then given by [Eq. 3 from 14]:

$$L = -d_{mem} \frac{1}{\cos(15°)\ln(T)} \qquad (2)$$

The resulting EALs for the Al 1s and Al 2p photoelectrons and both membranes are summarized in Fig 4 (filled squares and triangles).

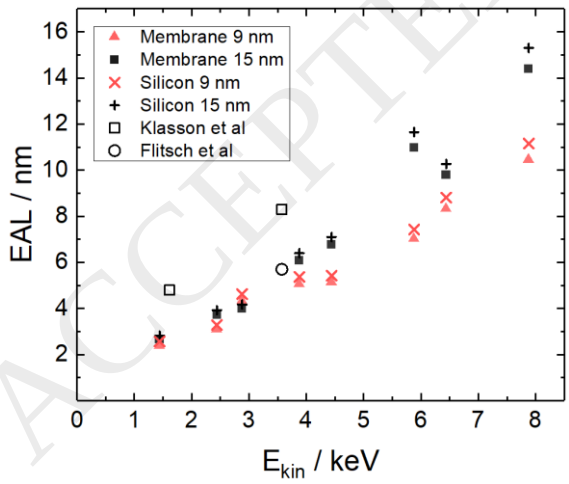

Figure 4. Electron effective attenuation length in the Si membrane(filled points) and effective attenuation length in silicon (crosses) after considering real sample structure for 9 nm (red) and 15 nm (black) membranes. Hollow points represent experimental data published by Klasson et al. [15] and Flitsch et al. [16].

The EALs of the 9 nm membrane mostly lie below the EALS of the 15 nm membrane, which might indicate a difference in the nominal thickness of the two membranes as compared to that provided by the supplier. The EALs values for both membranes align basically well with the exception of the two points at 5.88 keV and 7.88 keV for the 15 nm membrane, which are obtained from transmission values of Al 2s photoelectrons. This is most likely due to the underestimation of the plasmon contribution to the Y_m,[17] which had been discussed above. Also shown are the experimental values from the literature for effective attenuation length in silicon in the relevant energy range (hollow squares and circles). These values show significant scatter.

3.2 Determination of the effective attenuation length in silicon

The recorded spectra revealed that the silicon membrane and the Al film were oxidized (cf. Fig. 5) and also that some carbon impurities were present on both surfaces, i.e. the membrane and the Al film (cf. Fig. 6). This means, that the EAL values which we determined do not correspond directly to the EAL in silicon, but to a stack of silicon, silicon oxide and carbon.

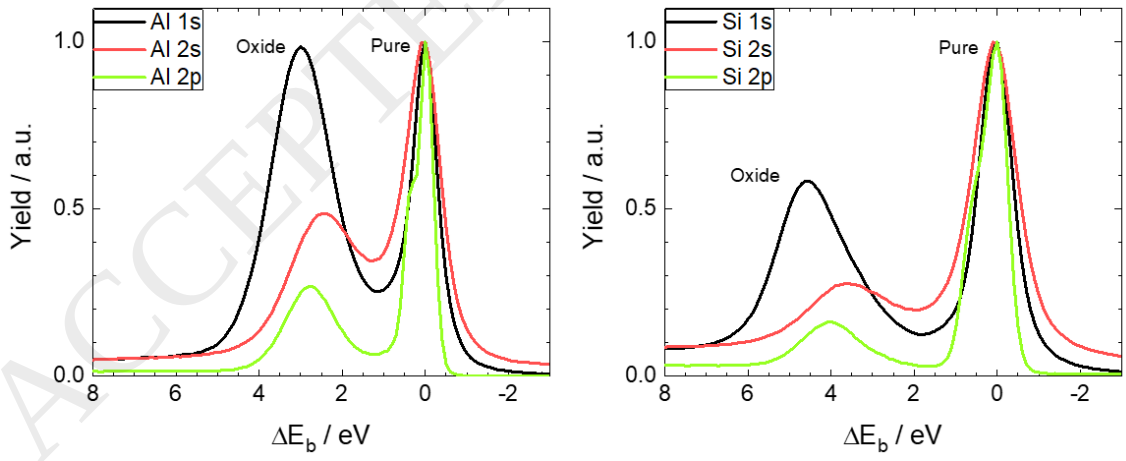

Figure 5. Al (left) and Si (right) 1s, 2s and 2p core levels for 3 keV excitation energy showing the intrinsic peak and a strong higher binding energy component due to oxidation. All spectra are normalized to the intrinsic (pure) peak.

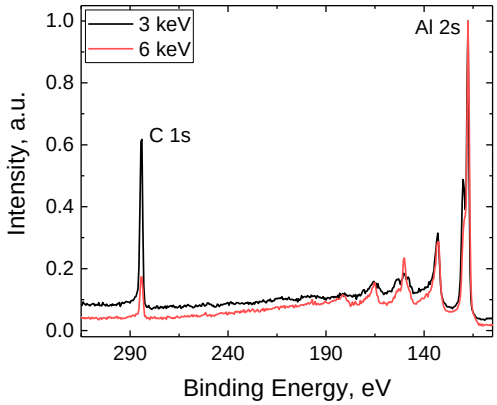

Figure 6: Spectra obtained with 3 keV and 6 keV excitation energy showing carbon contaminations on the aluminium film.

In order to obtain values for the EAL in silicon from the experimental EAL of the membrane, the modified transmission due to oxidation of the membrane and Al film as well as the carbon impurities on both surfaces needed to be taken into account. As we will see in the following, this resulted in only minor corrections, since the different influences largely cancelled each other. It is easily understood that, because a ratio of the yields $T = Y_m / Y_{AL}$ is used to calculate EAL, the influence of the carbon for instance will cancel out if the amount of carbon contamination is the same on the opposite sides of the sample. If not, depending whether the membrane or the Al has a thicker carbon layer, the EAL would be either under- or overestimated, respectively.

Al 1s and Al 2s spectra (see Fig. 5a) show high binding energy components indicating partial oxidation of the deposited film that were not present when the membrane was facing the CHA. This can be assigned to oxidation of the free surface of the Al film. This oxide layer increases the amount of scattering centres for escaping electrons. Therefore, the oxide film on the free surface of the Al decreases the amount of escaping photoelectron Y_{Al} leading seemingly to a higher T and thus an overestimation of the EAL in the silicon.

The Si 1s and 2s core levels also show a satellite at high binding energy, which indicates that the membranes are partially oxidised since they had been kept at ambient for considerable time. Contrary to the Al film, both sides of the membrane will be oxidized as both had been exposed to ambient.

The oxidation of the membranes increases their effective material thickness, thus decreases Y_m and consequently leads to an underestimation of the EAL.

From the above, and anticipating the result of the following analysis, it is already clear that the effect of carbon contaminations on both sides of the sample as well as the oxidation of membrane and Al film will largely cancel each other and thus any necessary correction to the EAL is thus expected to be small. We should note that in order to correct for the influence of the oxide and carbon layers we needed cross sections and IMFP values for these materials, i.e. SiO_2, Al and Al_2O_3. For that we resorted to the literature. Estimated elastic contribution to EAL for electrons (Eq. 5.13 in [7]) with 1.2 keV kinetic energy, close to the kinetic energy of Si 1s electrons at 3 keV excitation (E_{kin}=1.16 keV), traveling through Si and Al is 9.1% and 8.7%, respectively. For higher electron kinetic energies elastic contributions to the EAL are smaller and therefore, neglecting elastic contribution, we use IMFP values in the following estimation. The values for the IMFP in Si, Al and C (graphitic form) were taken from [4], for Al_2O_3 from [18] and for SiO_2 from [18] and [19]. Cross sections were taken from Scofield [1]. On the first view, resorting here to literature values appears to be inconsistent with our intent to accurately experimentally determine EAL values in silicon. However, because of the smallness of the overall corrections, as we will see, even large inaccuracies in the literature values would have comparably small influence on the accuracy of the determined EAL values in silicon.

In order to assess the influence of carbon and oxide layers on the determination of the effective attenuation length of silicon, it is necessary to estimate their thickness. We do so by considering the sample represented by the model shown in Fig. 7.

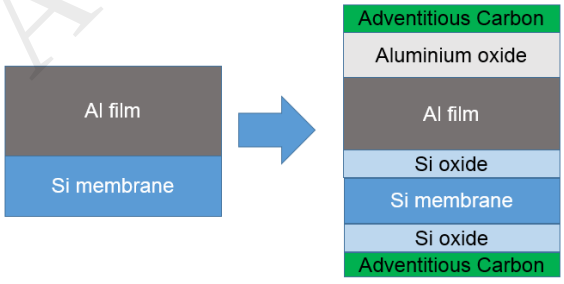

Figure 7. The ideal sample (left) and the real sample (right)

The yield of specific photoelectrons from a layer of material B of thickness d_B is given by:

$$Y_{B0} = Y_B^{\infty}\left(1 - \exp\left(-\frac{d_B}{\lambda_{B,B}}\right)\right)$$

where $Y_B^{\infty} \sim \sigma_B n_B \lambda_{B,B}$ is the corresponding photoelectron yield of the semi-infinite bulk material B. The yield is proportional to σ_B which is the photoionization cross section of the specific orbital from which the photoelectrons originate for the used X-ray energy, n_B is the concentration of the corresponding photoionization centres in material B and $\lambda_{B,B}$ is inelastic mean free path of these photoelectrons in material B. When these have to travel additionally through an overlayer of material A of thickness d_A, the yield Y_B decays exponentially with the thickness of the overlayer:

$$Y_B = Y_{B0}\exp\left(-\frac{d_A}{\lambda_{B,A}}\right)$$

where $\lambda_{B,A}$ is the inelastic mean free path of photoelectrons of material B in A. In the following exponential functions are denoted by $K_{B,A} = \exp\left(-\frac{d_A}{\lambda_{B,A}}\right)$.

For calculating the influence of the contamination layers, we need to consider at the most a three-layer model as shown in Fig. 8. Photoelectron yields detected by the CSA for each of the layers in Fig 8a are expressed by

$$Y_A = Y_A^{\infty}(1 - K_{A,A})$$

$$Y_B = Y_B^{\infty}(1 - K_{B,B})K_{B,A}$$

$$Y_C = Y_C^{\infty}(1 - K_{C,C})K_{C,B}K_{C,A}$$

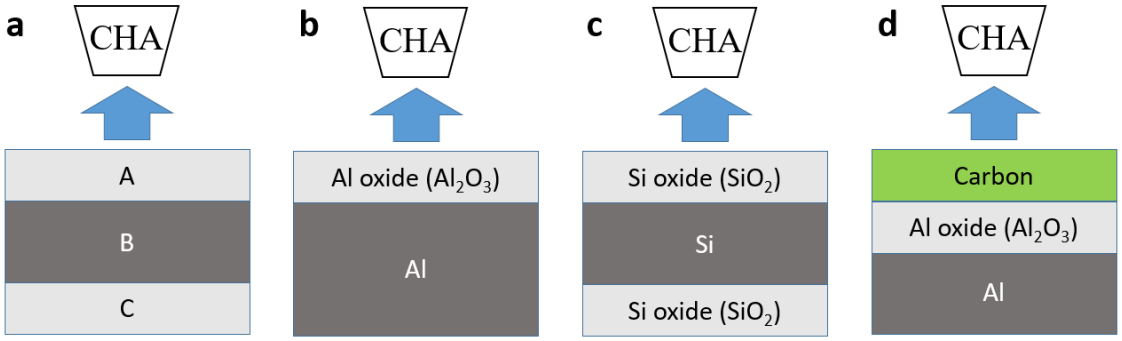

Figure 8. (a) photoelectrons emitted from a generic three layer structure to the photoelectron analyzer (CHA), (b) emission from a two layer structure to estimate the thickness of Al oxide, (c) a three layer structure to estimate Si oxide thickness and (d) a three layer structure to estimate the thickness of carbon layers. Al_2O_3 is present only on top of the Al film and carbon present only on both outer faces

For estimating the thickness of Al oxide on the Al film, some approximations are used. We neglect the difference in photoelectron kinetic energy between Al 1s and Al 2s core levels emitted from Al and its oxide since it is less than 0.5%. Their inelastic mean free path is thus taken the same and depends only on the material they travel through. As a consequence for the ratio of the yields of the photoelectrons travelling through the Al oxide to the yield of the photoelectrons travelling through the Al i.e. Y_{Alox}/Y_{Al}, the thickness of the carbon layer is irrelevant.

It is obvious that the thickness of the Al film decreases proportionally to the amount of Al used to create the aluminium oxide, hence $K_{Al,Al} = \exp(-\frac{d_{Al}-d_{Alox}}{\lambda_{Al,Al}})$, where d_{Al} is the film thickness measured right after the deposition. The photoelectron yields originating from the Al-oxide Y_{Alox} and from the Al Y_{Al} are given by

$$Y_{Alox} = Y_{Alox}^{\infty}(1 - K_{Al,Alox})$$

$$Y_{Al} = Y_{Al}^{\infty}(1 - K_{Al,Al})K_{Al,Alox}$$

Dividing Y_{Alox} by Y_{Al} and rearranging the terms gives:

$$1 - K_{Al,Alox} - Y_R \frac{Y_{Al}^{\infty}}{Y_{Alox}^{\infty}}\left(1 - K_{Al,Al}\right)K_{Al,Alox} = 0 \qquad (3),$$

where $Y_R = \frac{Y_{Alox}}{Y_{Al}}$, The two yields Y_{Alox} and Y_{Al} were obtained from fitting the oxide and metallic components of Al photoelectron peak. We determined the oxide thickness d_{Alox}, which enters into equation (1) as a part of the exponents $K_{Al,Al}$, $K_{Al,Alox}$ by graphically solving equation 1. The resulting values of Al oxide for 9 nm and 15 nm membranes are shown in Table I.

Table I. Oxide thickness on Al film and Si membrane. Si oxide thickness is calculated using the IMFP data from Akkerman et al. [18] (Akk) and Ashley et al. [19] (Ash) and the average of both (av).

	d_{Al2O3}/nm	d_{SiO2}/nm (Akk)	d_{SiO2}/nm (Ash)	d_{SiO2}/nm (av)
15 nm	4.08	6.06	5.92	5.99
9 nm	4.06	4.87	4.80	4.84

The thickness of silicon oxide d_{Siox} (see Fig. 5b) is estimated following the same procedure. Because of the small difference in kinetic energy, photoelectrons from the oxide and intrinsic component are assumed to have the same EAL (in the same material). We also assume that both sides of the membrane are covered by silicon oxide of the same thickness $d_{SioxA} = d_{SioxC}$, therefore $K_{SioxA,SioxA} = K_{SioxA,SioxC} = K_{SioxC,SioxA} = K_{SioxC,SioxC}$ and are denoted as $K_{Si,Siox}$.

The yields for each of the three layers are thus expressed as

$$Y_{SioxA} = Y_{Siox}^{\infty}(1 - K_{Si,Siox})$$

$$Y_{Si} = Y_{Si}^{\infty}(1 - K_{Si,Si})K_{Si,Siox}$$

$$Y_{SioxC} = Y_{Siox}^{\infty}(1 - K_{Si,Siox})K_{Si,Si}K_{Si,Siox}$$

Dividing $(Y_{SioxA}+Y_{SioxC})/Y_{Si}$ and rearranging the terms gives the equation

$$1 - K_{Si,Siox} + (1 - K_{Si,Siox})K_{Si,Si}K_{Si,Siox} - Y_R\frac{Y_{Siox}^{\infty}}{Y_{Si}^{\infty}}(1 - K_{Si,Si})K_{Si,Siox} = 0 \quad (4),$$

where $Y_R = \frac{Y_{Siox}}{Y_{Si}} = \frac{Y_{SioxA}+Y_{SioxC}}{Y_{Si}}$ with Y_{Siox} and Y_{Si} obtained from fitting the oxide and metallic components of Si photoelectron peak. The values of Si oxide resulting from solution of Eq. 2 for 9 nm and 15 nm membranes were again obtained graphically and are shown in Table I.

Next we estimate the thickness of the carbon impurity d_C on Al film side and on the membrane side of the samples.

$$Y_C = Y_C^{\infty}(1 - K_{C,C}) \quad (3)$$

The Al and Alox yields (film side) will be attenuated by $K_{Al,C}$, while Siox and Si yields (membrane side) will be attenuated by $K_{Si,C}$.

For the case of Al film side of the sample the carbon thickness d_C will be given by the solution to the equation:

$$1 - K_{C,C} - Y_R \frac{Y_{Alox}^{\infty}}{Y_C^{\infty}} \left(1 - K_{Al,Alox}\left(1 - \frac{Y_{Al}^{\infty}}{Y_{Alox}^{\infty}} + \frac{Y_{Al}^{\infty}}{Y_{Alox}^{\infty}} K_{Al,Al}\right)\right) K_{C,C} = 0$$

Here $Y_R = \frac{Y_C}{Y_{Al}+Y_{Alox}}$ with the integral yields Y_C, Y_{Al} and Y_{Alox} being obtained from the photoelectron spectra by peak fitting of the respective component. An equivalent equation is obtained for the case of the carbon impurity on the membrane side of the sample. The resulting values for carbon thickness d_C for both sides of the 9 nm and 15 nm membranes are shown in Table II.

Table II. Carbon thickness on the membrane side d_{mC} and on the Al film side d_{AlC}.

membrane	d_{AlC} / nm	d_{mC} / nm	d_{AlC}-d_{mC} / nm
15 nm	0.59	0.27	0.32
9 nm	0.36	0.29	0.07

The EAL values, determined by including all the above-mentioned corrections, are shown in Fig. 2 as red and black crosses, for 9 nm and 15 nm membranes respectively.

As already indicated above, the whole procedure resulted in only minor changes to the raw data. The relative difference between the EAL values of the membrane stack (Fig. 7) and those of pure silicon is below 10%.

4 Discussion

Fig 9 compares the EAL values (red points) averaged for the two membranes with the EAL) values for Si from predictive formula of Seah [20] for unpolarized X-ray (solid black),

single scattering albedo approximation of Jablonski [21, configuration A] for polarized X-rays (solid red), as well as Si IMFP based on a Bethe equation fit (dashed black)from Tanuma et al [4]. To calculate the single scattering albedo for [20] IMFP values of Tanuma et al. [4] and transport cross-sections from the tabulated data of [22] were used. If the elastic scattering of the electrons is negligible, the EAL would be the same as the IMFP. It is interesting to note in this respect that in Fig. 9 the EAL and IMFP values, calculated using empirical equation proposed by [20] and [4], respectively, are crossing. This must mean that the energy dependence of the EAL or the IMFP is not predicted correctly at least by one of the two works. It should also be noted here that Jablonski and Powell [23] have found that predictive equation of Seah [20] has a higher RMS deviation in representing Monte Carlo simulated EALs than a single scattering albedo approximation of Tanuma et al. [7]. Our experimentally obtained EAL values lie below the calculated IMFP and EAL values. This could indicate that in particular the elastic scattering is underestimated by the empirical predictive formulae.

To compare the energy dependence of the experimentally obtained EAL with the one predicted we fitted the two curves and the data using the power law

$$\lambda = k\left(\frac{E}{keV}\right)^{p} \quad (5),$$

where λ is the characteristic length (i.e. EAL or IMFP). The resulting k and p are summarized in Table 3. The value of p obtained from the experimental data is 20%, 23% and 27% larger than that obtained from fitting the EAL of Seah [20] and Jablonski [21] and IMFP values from predictive formulae, respectively. The significant difference between the experimental data and the values calculated using the empirical formula of Seah [20], Jablonski [21] and Tanuma et al. [4] is caused largely by the pre-factor k, which differs by up to ~ 70%.

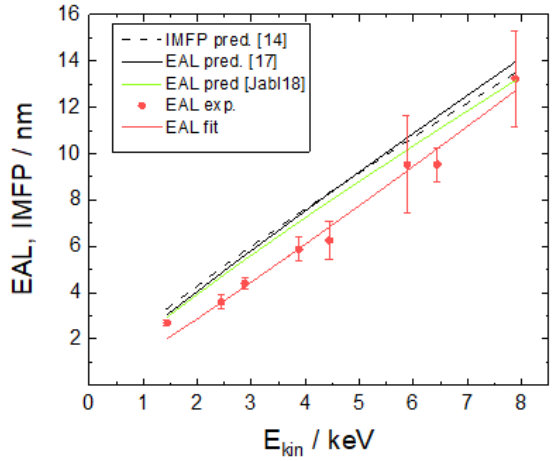

Figure 9. Experimentally determined effective attenuation length in silicon (experimental values – red points, power law fit – red solid line). For comparison effective attenuation length from [20] (black solid), from [21] (green solid) and inelastic mean free path (black dashed) from [4] are shown.

Table 3. Pre-exponential factor *k* and exponent power *p* for the power law fit (Eq. 4) to the predictive formulae from Seah et al. [20] (Seah), single-scattering albedo approximation of Jablonski [21] (Jablonski) and Tanuma et al. [4] (Tanuma) and experimental data.

	k/nm	*p*
EAL (Seah)[20]	2.16 +- 0.01	0.902 +- 0.003
EAL (Jablonski)[21]	2.14 +- 0.01	0.879 +- 0.001
IMFP (Tanuma)[4]	2.39 +- 0.01	0.837 +- 0.003
EAL exp	1.4 +- 0.2	1.08 +- 0.07

We believe that the use of membranes will become increasingly popular for (N)APPES investigations, using higher electron kinetic energies. In addition to higher electron kinetic energies it is also of advantage to employ higher X-ray excitation energies. The electron yield observed through a membrane is proportional to the transmission factor *T* multiplied by the photo excitation cross section σ_T. Thus, in an experiment, similar to the present one, but where we want to observe reactions of aluminium in an environment which is separated from the electron analyzer by the membrane, it is beneficial to rather detect the Al 1s level instead of the Al 2s level, because the higher cross section of the Al 1s level results in a strong gain in signal. This is shown in Fig. 10.

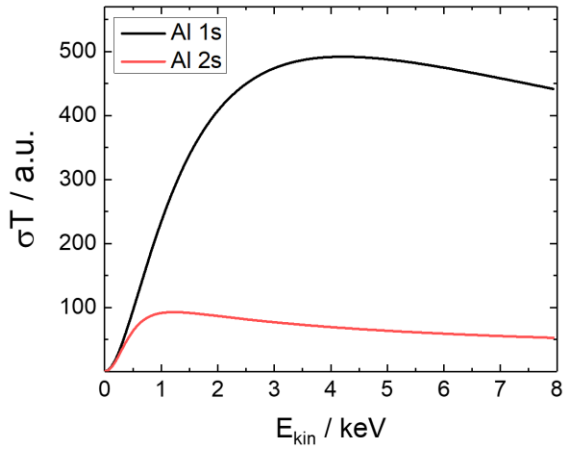

Figure 10. The product of the photoionization cross-section σ and measured transmission T for 15 nm membrane as a function of kinetic energy for Al 1s ((E_b = 1559.6 eV) and Al 2s (E_b = 117.8 eV) core levels; σT is proportional to the electron yield through the membrane. The photoinization cross section σ is taken from Scofield [1] for the corresponding X-ray excitation energy E_γ and subshell.

Important to mention, there may be another good reason to record deeper core levels in case we are interested in chemical changes of particular elements in near ambient environment, As Fig. 5 shows, the Al and the Si core levels show strong satellites as a result of oxidation. The deeper core levels of Si and Al obviously react more sensitively to the oxidation and show a significantly stronger chemical shift than the corresponding 2*s* and 2*p* signals. The shift between the metallic and oxide component amounts to 3.0 eV at E_γ = 3 keV for Al 1*s* compared to 2.5 eV for Al 2*s* or 2.7 eV for Al 2*p*. Consequently, the oxide component can also be better resolved when using higher X-ray energies. For the case of Si the respective oxide shifts are even more dramatic and amount to 4.6 eV for Si 1*s*, 3.6 eV for Si 2*s* and 4.0 eV for Si 2*p*. This finding is astonishing and contrary to the general belief that shallow levels should experience larger chemical shift. However, this assumption is largely based on simple charge transfer and screening model and neglects possible effects of re-hybridization.

Conclusion

In summary, we presented a new approach for determining the effective attenuation length for electrons in materials, which we used to determine the EAL of electrons in silicon with electron kinetic energies in the multi keV range. We also

showed how to correct for the influence of contamination layers and demonstrated that their overall effect on the accuracy of the method is small. The approach can be employed for other materials. It is better suited for photoelectrons with high (>> 1keV) kinetic energy since membranes with thickness >> 10 nm can be more easily prepared. Using thicker membranes also decreases uncertainties in the EAL due to surface contaminations. To facilitate the analysis, material for the film should be selected to avoid overlapping of the elastic peaks with the plasmon features of the membrane material.

We believe that experimental investigations of EAL at higher kinetic energies will become increasingly important because HAXPES investigation of materials is becoming increasingly popular. Furthermore, some of the approximations valid at moderate or intermediate electron kinetic energies may not hold any longer at high energies. For instance, at higher energies, above about $15Z^2$ eV, where Z is the atomic number of the element, the elastic scattering cross section should be better described by the Born approximation becoming ~ Z^2 [24].

Our experimental study also demonstrated that the application of hard X-ray excitation has some important advantages over classical soft X-ray approaches for photoelectron spectroscopy under (near) ambient conditions. Use of deeper core levels enhances cross sections and thus the photoelectron yield while also higher chemical sensitivity may be achieved.

Acknowledgement:

We gratefully acknowledge help of Ursula Kainz at Johannes Kepler University in preparation of the Al films and time at Diamond beamline I09 (proposal number NT-15716-1) with skilful assistance by David Duncan, Pardeep Kumar Thakur and Dave McCue. AW has received funding from the European Union's Horizon 2020 research and innovation programme under the Marie Skłodowska-Curie grant agreement (GA) No 665593 awarded to the Science and Technology Facilities Council. VS acknowledges financial support by the *Österreichische Akademie der Wissenschaften* through the DOC fellowship program.

References

[1] J. H. Scofield, Theoretical Photoionisation Cross Sections from 1 to 1500 keV, Lawrence Livermore National Laboratory, Report UCRL-51326, 1973.

[2] For orbitals with low binding energy (e.g. Au 5p/4f) in particular deviations from Scofield's calculations have been noted. See e.g.: *Outer Sub-Shell Cross-Sections Determined by X-ray Photoelectron Spectroscopy up to 14.5 keV; C. Kunz, S. Thiess, B.C.C. Cowie, T.-L. Lee, and J. Zegenhagen Nuclear Instruments and Methods A, 547 (2005) 73 - 86, DOI: 10.1016/j.nima.2005.05.014*

[3] https://www.nist.gov/srd/srd-catalog

[4] S. Tanuma, C. J. Powell, D. R. Penn, Surface and Interface Analysis, 43 (2011) 689-713, DOI: 10.1002/sia.3522

[5] A. Jablonski, F. Salvat and C. J. Powell, Journal of Physical and Chemical Reference Data, 33 (2004) 409-451, DOI: 10.1063/1.1595653

[6] A. Jablonski and C.J Powell, Journal of Electron Spectroscopy, 100 (1999) 137-160, DOI: 10.1016/S0368-2048(99)00044-4

[7] see e.g. C. J. Powell and S. Tanuma in Hard X-ray Photoelectron Spectroscopy (HAXPES) Volume 59 of the series Springer Series in Surface Sciences, edited by J. Woicik, pp 111-140

[8] C. Dallera, L. Duo, L. Braicovich, G. Panaccione, G. Paolicelli, B.C.C. Cowie, J. Zegenhagen, Applied Physics Letters, 85 (2004) 4532, DOI: 10.1016/j.nima.2005.05.017

[9] J. Zegenhagen, C. Kunz (Eds.), Proc. of the Workshop on Hard X-ray Photoelectron Spectroscopy, Grenoble 2003; Nuclear Instruments and Methods in Physics Research A 547(2005).

[10] Joseph C. Woicik (Ed.), Hard X-ray Photoelectron Spectroscopy (HAXPES), Springer Series in Surface Sciences, Springer Cham Heidelberg New York Dordrecht London (2016).

[11] P. Risterucci, O. Renault, E. Martinez, B. Detlefs, V. Delaye, J. Zegenhagen, C. Gaumer, G. Grenet and S. Tougaard, Applied Physics Letters, 104 (2014) 051608-051608.4, DOI: 10.1063/1.4864488

[12] A similar approach to determine the EAL of electrons had been used more than fifty years ago: V. E. Cosslett and R. N. Thomas, Br. J. Appl. Phys. 15 (1964) 883; DOI: 10.1088/0508-3443/15/8/303

[13] See e.g.: D. E. Starr, M. Favaro, F. F. Abdi, H. Bluhm, E. J. Crumlin, Roel van de Krol, Journal of Electron Spectroscopy and Related Phenomena, 221 (2017) 106-115, DOI: 10.1016/j.elspec.2017.05.003

[14] C. J. Powell and A. Jablonski, Surface and interface analysis, 33 (2002) 211-229, DOI: 10.1002/sia.1204

[15] M. Klasson, A. Berndtsson, J. Hedman, R. Nilsson, R. Nyholm, C. Nordling, Journal of Electron Spectroscopy and Related Phenomena, 3 (1974) 427-434, DOI: 10.1016/0368-2048(74)80029-0

[16] R. Flitsch and S. I. Raider, Journal of Vacuum Science and Technology, 12 (1975) 305-308, DOI: 10.1116/1.568771

[17] The excitation probability of extrinsic plasmons must be the same because of only maximal ≈ 1% difference in kinetic energy for 2s and 2p photoelectrons. However, intrinsic plasmons excited immediately by the Si 2s and 2p photoelectrons while leaving the atom may contribute differently to the total Si 2s and 2p plasmon yield.

[18] A. Akkerman, T. Boutboul, A. Breskin, R. Chechik, A. Gibrekhterman, Y. Lifshitz, Physica Status Solidi (b), 198 (1996) 769-784, DOI: 10.1002/pssb.2221980222

[19] J. C. Ashley and V. E. Anderson, Journal of Electron Spectroscopy and Related Phenomena, 24 (1981) 127-148, DOI: 10.1016/0368-2048(81)80001-1

[20] M. P. Seah, Surface and Interface Analysis, 44 (2012) 1353–1359, DOI: 10.1002/sia.5033

[21] A. Jablonski, Surface Science, 667(2018) 121-137, DOI: 10.1016/j.susc.2017.10.008

[22] R. Mayol and F. Salvat, Atomic Data and Nuclear Data Tables, 65 (1997) 55-154. DOI: 10.1006/adnd.1997.0734

[23] A. Jablonski and C.J. Powell, Journal of Electron Spectroscopy and Related Phenomena, 199 (2015) 27-37, DOI: 10.1016/j.elspec.2014.12.011

[24] H.A. Bethe and R.W. Jackiw, Intermediate Quantum Mechanics, Benjamin, New York, 1968.